Dalton Transactions

ROYAL SOCIETY OF CHEMISTRY

COMMUNICATION

View Article Online
View Journal | View Issue

Check for updates

Cite this: *Dalton Trans.*, 2022, **51**, 9591

Received 9th March 2022,
Accepted 31st May 2022

DOI: 10.1039/d2dt00743f

rsc.li/dalton

An isoindoline bridged $[M(\eta^6\text{-arene})_2]^+$ (M = Re, ^{99m}Tc) *ansa*-arenophane and its dinuclear macrocycles with axial chirality†

Joshua Csucker, Da Kyung Jo, Qaisar Nadeem, Olivier Blacque, Thomas Fox, Henrik Braband and Roger Alberto *

This work presents a straightforward method for the preparation of an isoindoline bridged $[M(arene)_2]^+$ (M = Re, ^{99m}Tc) *ansa*-[3]arenophane. This intramolecular formation of an *ansa*-complex is accompanied by the intermolecular formation of a pair of isoindoline bridged macrocyclic dinuclear sandwich complexes, one of which exhibits axial chirality.

Introduction

Cyclopentadienyl-based *ansa*-metallocenes and arene-based [*n*]arenophanes (*n* = number of bridging atoms) are the backbone of olefin polymerization and other catalytic processes.[1] *Ansa*-derivatives of ferrocene and group 4 elements have been studied particularly extensive due to their impressive chemical and catalytic diversity.[1–4] There is a plethora of literature precedence for late transition metal *ansa*-complexes[5] including group 7 elements.[6] *Ansa*-rhenocene complexes with Re^{III} were reported by Heinekey *et al.*[7] and Conway and coworkers.[8] They reported the synthesis of $C(CH_3)_2$ and $Si(CH_3)_2$ bridged rhenocenes respectively. These interesting compounds suffer though from shortcomings; *e.g.* the $Si(CH_3)_2$ bridged compound is thermally unstable at room temperature ($t_{1/2}$ = 2 h) and decomposes under methane elimination. The $C(CH_3)_2$ linked complex can only be isolated in very low yields. *Ansa*-[*n*]arenophanes are far less known and mainly reported since their discovery by Schneider *et al.* in the 1990s[9] for group 6 and for group 8 elements.[10] They are unknown at all for rhenium and technetium thus far and represent an unanswered challenge. Given the existence of arenophanes with group 6 *ansa*-metallocenes and *ansa*-[*n*]arenophane with group 8 elements, stable group 7 *ansa*-[*n*]arenophanes would fill a knowledge gap.

Department of Chemistry, University of Zurich, Winterthurerstrasse 190, CH-8057 Zurich, Switzerland. E-mail: ariel@chem.uzh.ch

† Electronic supplementary information (ESI) available. CCDC 2142820–2142823. For ESI and crystallographic data in CIF or other electronic format see DOI: https://doi.org/10.1039/d2dt00743f

An attractive entry into *ansa*-chemistry is the $[M(\eta^6\text{-arene})_2]^+$ (M = Re, ^{99m}Tc) family of compounds. These cationic, arene-based sandwich complexes are water-soluble and air- and moisture stable. Alkyl derivatized $[Re(\eta^6\text{-arene})_2]^+$ complexes can directly be synthesized from $Na[ReO_4]$ under Fischer–Hafner conditions.[11,12] Lithiation of $[Re(\eta^6\text{-}C_6H_6)_2]^+$ and quenching with electrophiles leads to an array of mono- and bis-substituted compounds.[13–18] Alternatively, naphthalene in $[Re(\eta^6\text{-napht})_2]^+$ can be exchanged by functionalized arenes with a high degree of functional group tolerance.[15,18]

Technetium chemistry is developed *in tandem* with the one of rhenium. ^{99m}Tc complexes are of special interest for diagnostic, medicinal chemistry due to their potential application as radio-pharmaceuticals.[19,20] A distinct advantage of $[^{99m}Tc(\eta^6\text{-arene})_2]^+$ complexes is their direct synthesis in water and under mild conditions with vast substrate scope.[15,18,21]

We present in this report the first example of stable $[M(\eta^6\text{-arene})_2]^+$ (M = Re, ^{99m}Tc) type *ansa*-complex, featuring an isoindoline unit as the bridge between the two arene ligands, and an uncommon dinuclear macrocycle formed by intermolecular isoindoline formation starting from $[Re(\eta^6\text{-}C_6H_5\text{-}NH_2)_2]^+$.

Results and discussion

Since the aforementioned silyl- or carbon-bridged *ansa*-metallocenes of Re^{III} are temperature, oxygen and moisture sensitive, we hypothesized that *ansa*-[*n*]arenophanes would be more persistent. We targeted to exploit the literature reported condensation reaction between 2 eq. of aniline or amino pyridines and *ortho*-phenyldialdehyde (OPA) which is known to form heterocyclic isoindolines units in a straight-forward manner (Scheme 1, left).[22–24] We rationalized that a 1,1′-diamino sandwich complex might replace the individual anilines in the organic template reaction to form the corresponding *ansa*-complex. With $[M(aniline)_2]^+$ (M = Re: $[\mathbf{4}]^+$; M = ^{99m}Tc: $[\mathbf{7}]^+$) as synthetic precursor an isoindoline-bridged *ansa*-[3]arenophane should be accessible by treatment with OPA (Scheme 1).

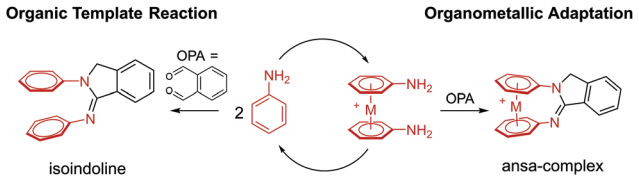

Scheme 1 Concept for the synthesis of novel isoindoline bridged *ansa*-complexes. OPA = *ortho*-phenyldialdehyde; M = Re, ^{99m}Tc.

Complex [**4**][PF_6] was prepared *via* two different synthetic routes (Scheme 2). Starting from [**1**][PF_6], [**4**][PF_6] can be obtained in 21% yield over two steps according to a literature procedure by arene exchange of naphthalene with aniline.[15] The literature yields were improved from 39 to 88% by employing a large excess of aniline as compared to the literature report. An alternative route is an adapted Gabriel amine synthesis inspired by the preparation of 1,1′-diaminoferrocene as reported by Abdulmalic and Rüffer.[25] Bis-chlorinated [**2**][PF_6][17] was treated with potassium phthalimide (KPhth) in the presence of copper to provide [**3**][PF_6] in excellent yields (97%). The X-ray structure of [**3**][PF_6] was elucidated (ESI, Fig. S24†). Hydrazine mediated phthalimide elimination delivered [**4**][PF_6] in a satisfactory yield of 65% (Scheme 2).

Complex [**4**][PF_6] was treated with stoichiometric amounts of OPA (Scheme 2), which provided the *ansa*-complex [**5**][TFA] in 25% yield. Additionally, two dinuclear macrocyclic complexes, [**6a**][TFA]$_2$ and [**6b**][TFA]$_2$ were isolated in a combined yield of 62% and in a 2.75 : 1 molar ratio according to ^{1}H NMR data (ESI Fig. S7–S15†). Increasing the dilution of the reagents distinctly favors the formation of [**5**]$^+$, albeit with sustained observation of the dinuclear species. At extremely high dilution, as in case of ^{99m}Tc (*vide infra*), exclusively the monomer is observed. All products were characterized by NMR, FT-IR, HR-ESI-MS, elemental analysis (EA) and single crystal X-ray diffraction (ESI, Fig. S17–S23 and S25–27†). Due to the hygroscopic nature of the TFA salts, the compounds were converted to the respective PF_6^- salts for EA measurements.

The formation of [**5**]$^+$ was monitored over the course of the reaction by UPLC-ESI-MS. Based on results thus obtained, we

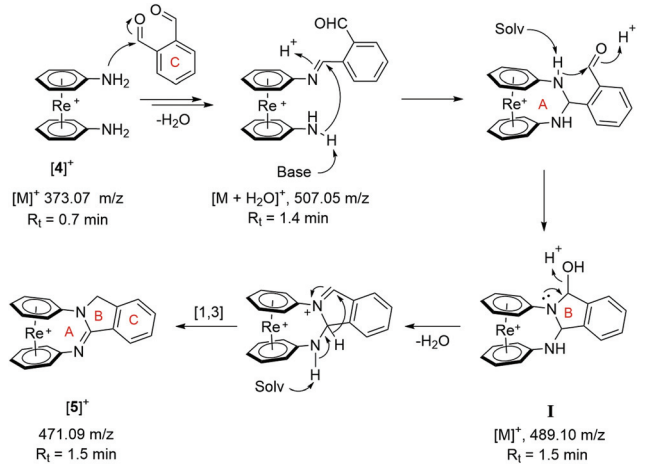

Scheme 3 Mechanistic reaction scheme of the formation of [**5**]$^+$ from [**4**]$^+$. Indicated *m*/*z* values and retention times (Rt) correspond to observed intermediates.

propose a step-by-step mechanism shown in Scheme 3. This proposal is based on a similar pathway as described by Chebolu *et al.* for the synthesis of 1,2-disubstituted benzimidazoles.[22] Two possible routes lead to the *ansa*-species [**5**]$^+$, namely formation of a symmetrical di-imine followed by cyclization or a sequence of mono-imine formation followed by a sigmatropic rearrangement. According to our data, the second pathway is more likely to be at play. Imine formation between [**4**]$^+$ and OPA (observed as [M + H_2O]$^+$; *m*/*z* = 507.05) followed by nucleophilic attack of the second aniline nitrogen generates the A ring. Subsequent imine formation between the secondary amine and the remaining aldehyde moiety results in the fused A–B–C ring system, supported by the observation of the key intermediate **I**. Elimination of water and rapid [1,3] sigmatropic rearrangement finally delivers [**5**]$^+$. The dinuclear species [**6a**]$^{2+}$ and [**6b**]$^{2+}$ are the result of intermolecular imine formations instead of an intramolecular pathway. A detailed overview of all observed intermediates and pathways is provided in the ESI (Scheme S1†).

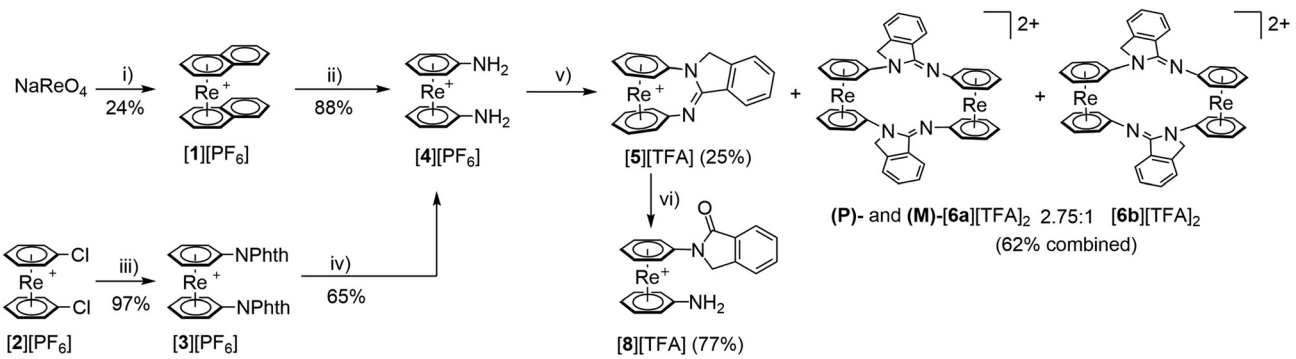

Scheme 2 Overall synthetic route to the *ansa*-complex [**5**]$^+$ and the dinuclear species [**6a**]$^{2+}$ and [**6b**]$^{2+}$. Reaction conditions: (i) Zn, $AlCl_3$, naphthalene, 100 °C, 18 h; (ii) aniline, *N*-methyl pyrrolidone, 1,4-dioxane, 120 °C, 4 h; (iii) Cu turnings, potassium phthalimide, THF, 70 °C, 22 h; (iv) aq. hydrazine, CH_3CN, 25 °C, 24 h, (v) OPA, 0.1 vol% TFA in H_2O, CH_3CN, 25 °C, 2 h, then 80 °C, 3.6 h; (vi) conc. HCl, 70 °C, 24 h.

Complex [**5**][PF_6] crystallized in the monoclinic space group $P2_1/c$ with one CH_3CN solvent molecule in the asymmetric unit (Fig. 1). The centroid–Re–centroid angle (169.66(7)°) is significantly smaller than the optimal 180° but still larger than the one reported by Heinekey *et al.* for their *ansa*-rhenocene (145.2(16)°).[7] The angle between the η^6-C_6H_6 planes is 15.23(9)°, indicating an exposure of the rhenium center. The arene ligands are in an almost perfectly eclipsed conformation. The bridging isoindoline unit is arranged perpendicular to the π-surfaces of the sandwich scaffold.

We were interested in reactivities of [**5**]$^+$, particularly in the question if oxidative addition to the exposed rhenium center would occur, given the strain imposed on the arene ligands by the bridging isoindoline. Such reactivities would be desirable if the *ansa*-complexes were supposed to enter some catalytic processes. For their application in radiopharmacy, however, any metal-based reactivity has to be omitted. Treatment of [**5**][TFA] with CH_3I however did not lead to an oxidative addition and reaction with HBF_4 did not lead to rhenium protonation. Clean hydrolysis of the imine was observed with aqueous acids (77% yield, see ESI†) to yield compound [**8**][TFA]. This reaction is however, ligand-rather than metal-based. The strain of the arene ligands is thus too small to expose the rhenium center and facilitating *e.g.* oxidative addition reactions.

Analytically pure samples of [**6a**][$TFA]_2$ were obtained by fractional crystallization. Complex [**6b**][$TFA]_2$ could not be fully separated from [**6a**][$TFA]_2$. A structure elucidation revealed axial chirality[26] in [**6a**]$^{2+}$, thus both (*P*)- and (*M*)-enantiomers are present in the crystals as evident from a combination of NMR and crystallographic data. Moreover, classical coalescence behavior of the ^{1}H NMR signals was observed between 270 K and 330 K (ESI, Fig. S28†). This coalescence process describes the rapid interconversion between (*P*)- and (*M*)-enantiomers of [**6a**]$^{2+}$. The process has a free activation energy barrier of $\Delta G^{\ddagger}$ = 64.0 ± 0.4 kJ mol^{-1}, which corresponds to a first order rate constant k = 65.76 s^{-1} at 298 K (ESI chapter 4†). The best estimate for the coalescence temperature is 323 K. Thus, the solution structure of [**6a**]$^{2+}$ at room temperature is described as a rapid equilibrium between its enantiomers. In combination with ROESY correlation data (ESI, Fig. S31†), we assessed that only [**6a**]$^{2+}$ but not [**6b**]$^{2+}$ is involved in the coalescence behavior. The crystallographic data of [**6a**][$TFA]_2$ confirmed the axial chirality and the presence of a racemate (Fig. 2). It crystallized in the centrosymmetric space group $C2/c$ and the two rhenium centers lie on a two-fold axis. The asymmetric unit features both helical enantiomers. We assigned the (*P*)- and (*M*)-enantiomers based on rotational direction of the head-to-head oriented helices.[26] Bond lengths and angles of the isoindoline units are in the same range as those of [**5**][PF_6]·CH_3CN. The crystal structure of [**6b**][$TFA]_2$ shows a flytrap-like head-to-tail geometry of the two isoindoline-units bridging the two [$Re(\eta^6C_6H_6)_2]^+$ scaffolds (Fig. 1).

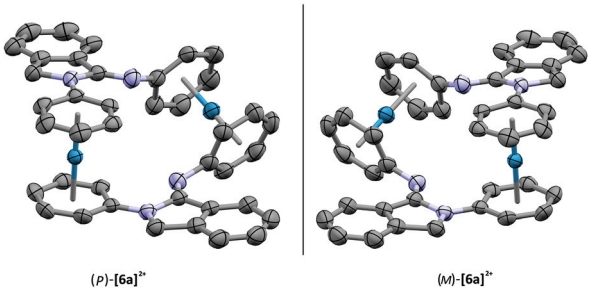

Fig. 2 Side-by-side ORTEP representations of the cations (*P*)-[**6a**]$^{2+}$ (left) and (*M*)-[**6a**]$^{2+}$of the crystal structure [**6a**][$TFA]_2$·H_2O. Counterions, hydrogen atoms and labels were omitted for clarity.‡ The black bar represents the mirror plane relating the two enantiomers.

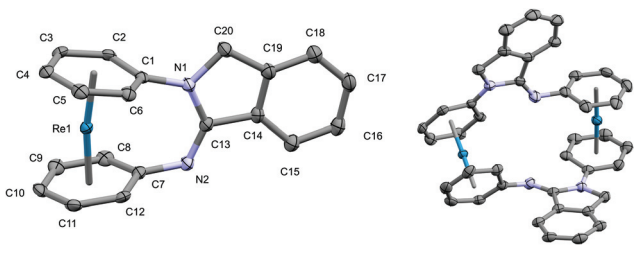

Fig. 1 ORTEP representation of the cations [**5**]$^+$ of the crystal structure [**5**][PF_6]·CH_3CN (left), and [**6b**]$^{2+}$ of the crystal structure [**6b**][$TFA]_2$·$2H_2O$ (right). Thermal ellipsoids represent 50% probability. Hydrogens and counterions were omitted for clarity.‡

It was tempting to investigate, if ^{99m}Tc would yield the same *ansa*-[*n*]arenophane complex directly in water and despite the presence of water, which affects imine formation. To verify this hypothesis, the same route as with rhenium was employed. Aqueous [$^{99m}TcO_4]^-$ was treated with aniline and zinc (impossible for Re) in saline which produced exclusively [^{99m}Tc(η^6-aniline)$_2]^+$ ([**7**]$^+$, Scheme 4).[15] To remove excess aniline, the crude reaction mixture was purified *via* HPLC and peaks containing [**7**]$^+$ collected. The resulting solution was treated with OPA which gave the ^{99m}Tc homologue *ansa*-complex [^{99m}Tc][**5**]$^+$ in a clean reaction. Complex [^{99m}Tc][**5**]$^+$ was isolated in excellent radiochemical purity of >98% after HPLC purification. Its chemical identity was confirmed by chromatographic coinjection with the rhenium homologue [**5**][TFA] (Fig. 3). Complex [^{99m}Tc][**5**]$^+$ represents the first example of a technetium *ansa*-complex. Although a two-step reaction, it is amazing that this kind of structurally diverse complexes can be prepared in water and in good yields. Analysis of the reaction solution did not indicate the formation

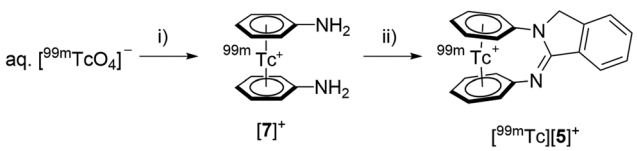

Scheme 4 Synthesis of the ^{99m}Tc *ansa*-complex [^{99m}Tc][**5**]$^+$. Reaction conditions: (i) zinc, aniline, 100 °C, 30 min, microwave; (ii) OPA, 80 °C, 40 min.

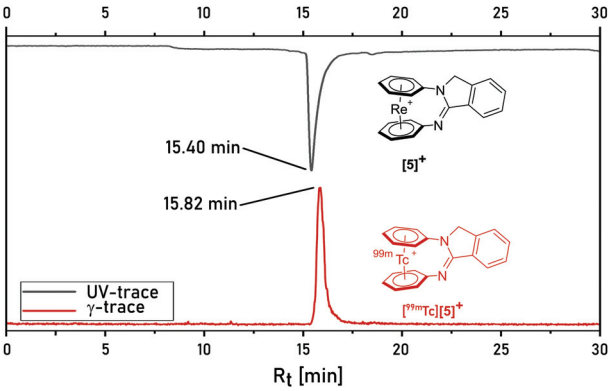

Fig. 3 Coinjection of $[^{99m}Tc][5]^+$ (red) with $[5]^+$ (black). The difference in retention times is associated with the dead volume between UV cell and radio detector.

of dinuclear species, analogous to $[\mathbf{6a}]^{2+}$. The high dilution of ^{99m}Tc (around 10^{-8} M) would require an extremely fast process to form dinuclear species, which appeared not to be the case with the reaction between $[7]^+$ and OPA.[27]

Especially the well-established synergy between rhenium and technetium renders the presented compounds interesting candidates for the development of chemical and radioactive probes.

Conclusions

We report the first examples of *ansa*-$[M(\eta^6\text{-arene})_2]^+$ (M = Re, ^{99m}Tc) complexes, featuring an isoindoline as the bridging unit. The high degree of stability coupled with the biorelevant properties of the isoindoline unit[24] renders [5][TFA] an attractive candidate as building block for bioorganometallic chemistry. The 1,2-dialdehyde unit can thereby act as an anchoring group to an active pharmaceutical or be even part of it. The fact that the analogous ^{99m}Tc complex is readily available further underlines the potential of the system in a radiopharmaceutical context. We assess that further exposure of the rhenium is required to explore eventual catalytic applications of $[5]^+$ and therefore, a more straining bridging unit is required.

Moreover, two dinuclear macrocyclic complexes, featuring comparably rare axial chirality for dinuclear species, were isolated and fully characterized. Perspective studies of the dinuclear species point to the preparation of heteronuclear Re–^{99m}Tc dimers to probe them as potential theranostic pairs.

Author contributions

JC wrote and edited the manuscript, conceptualized the project and performed experiments, DKJ performed experiments and edited the initial manuscript, QN performed ^{99m}Tc chemistry, OB performed all crystallographic measurements, TF recorded NMR spectra of $[\mathbf{6a}][TFA]_2$ at various temperatures, HB advised ^{99m}Tc experiments, RA revised the manuscript and initiated the project.

Conflicts of interest

There are no conflicts to declare.

Acknowledgements

The authors acknowledge financial support from the University of Zurich.

Notes and references

‡ The crystallographic data is available in the electronic ESI.†

1 B. Wang, *Coord. Chem. Rev.*, 2006, **250**, 242–258.
2 M. A. Bau, S. Wiesler, S. L. Younas and J. Streuff, *Chem. – Eur. J.*, 2019, **25**, 10531–10545.
3 L. N. Jende, A. Vantomme, A. Welle, J.-M. Brusson, J.-F. Carpentier and E. Kirillov, *J. Organomet. Chem.*, 2018, **878**, 19–29.
4 J. Kuwabara, D. Takeuchi and K. Osakada, *ChemComm*, 2006, 3815–3817.
5 T. Arnold, H. Braunschweig, A. Damme, C. Hörl, T. Kramer, I. Krummenacher and J. Mager, *Organometallics*, 2014, **33**, 1659–1664.
6 H. Braunschweig, A. Damme, K. Dück, M. Fuß, C. Hörl, T. Kramer, I. Krummenacher, T. Kupfer, V. Paprocki and C. Schneider, *Chem. – Eur. J.*, 2015, **21**, 14797–14803.
7 D. M. Heinekey and C. E. Radzewich, *Organometallics*, 1999, **18**, 3070–3074.
8 S. L. J. Conway, L. H. Doerrer, J. C. Green, M. L. H. Green, A. Scottow and A. H. H. Stephens, *J. Chem. Soc., Dalton Trans.*, 2000, 329–333.
9 J. J. Schneider, N. Czap, D. Spickermann, C. W. Lehmann, M. Fontani, F. Laschi and P. Zanello, *J. Organomet. Chem.*, 1999, **590**, 7–14.
10 D. Seyferth, *Organometallics*, 2002, **21**, 2800–2820.
11 E. O. Fischer and A. Wirzmüller, *Chem. Ber.*, 1957, **90**, 1725–1730.
12 E. A. Trifonova, D. S. Perekalin, K. A. Lyssenko and A. R. Kudinov, *J. Organomet. Chem.*, 2013, **727**, 60–63.
13 G. Meola, H. Braband, P. Schmutz, M. Benz, B. Spingler and R. Alberto, *Inorg. Chem.*, 2016, **55**, 11131–11139.
14 G. Meola, H. Braband, D. Hernández-Valdés, C. Gotzmann, T. Fox, B. Spingler and R. Alberto, *Inorg. Chem.*, 2017, **56**, 6297–6301.
15 Q. Nadeem, G. Meola, H. Braband, R. Bolliger, O. Blacque, D. Hernández-Valdés and R. Alberto, *Angew. Chem., Int. Ed.*, 2020, **59**, 1197–1200.
16 D. Hernández-Valdés, R. Fernández-Terán, B. Probst, B. Spingler and R. Alberto, *Helv. Chim. Acta*, 2020, **103**, e2000147.

17 D. Hernández-Valdés, F. Avignon, P. Müller, G. Meola, B. Probst, T. Fox, B. Spingler and R. Alberto, *Dalton Trans.*, 2020, **49**, 5250–5256.
18 Q. Nadeem, F. Battistin, O. Blacque and R. Alberto, *Chem. – Eur. J.*, 2022, **28**, e202103566.
19 A. G. Jones, *Radiochim. Acta*, 1995, **70–71**, 289–298.
20 U. Mazzi, R. Schibli, H.-J. Pietzsch, J.-U. Künstler and H. Spies, in *Technetium-99m Pharmaceuticals: Preparation and Quality Control in Nuclear Medicine*, ed. I. Zolle, Springer Berlin Heidelberg, Berlin, Heidelberg, 2007, pp. 7–58.
21 M. Benz, H. Braband, P. Schmutz, J. Halter and R. Alberto, *Chem. Sci.*, 2015, **6**, 165–169.
22 R. Chebolu, D. N. Kommi, D. Kumar, N. Bollineni and A. K. Chakraborti, *J. Org. Chem.*, 2012, **77**, 10158–10167.
23 S. S. Al-Shihry, *Molbank*, 2005, **2005**, M447.
24 I. Sović, S. Kraljević Pavelić, E. Markova-Car, N. Ilić, R. Nhili, S. Depauw, M.-H. David-Cordonnier and G. Karminski-Zamola, *Eur. J. Inorg. Chem.*, 2014, **87**, 372–385.
25 M. A. Abdulmalic and T. Rüffer, *Bull. Chem. Soc. Jpn.*, 2013, **86**, 724–728.
26 M. Rickhaus, M. Mayor and M. Juríček, *Chem. Soc. Rev.*, 2016, **45**, 1542–1556.
27 R. Bolliger, A. Frei, H. Braband, G. Meola, B. Spingler and R. Alberto, *Chem. – Eur. J.*, 2019, **25**, 7101–7104.